Weekly Report 03/19/25-03/26/25

Giovanni Michel

Northwestern

This Week

- Redid report from February 17^{th} .
- Made plots for $g_m(T)$ with the data I had. Will do $C(T)$ next.
- Next Week: Send email to Davide for progress update.
  - Meet with Matt to do grounding scheme for cryo-transistors.

Plots for $g_m(T)$

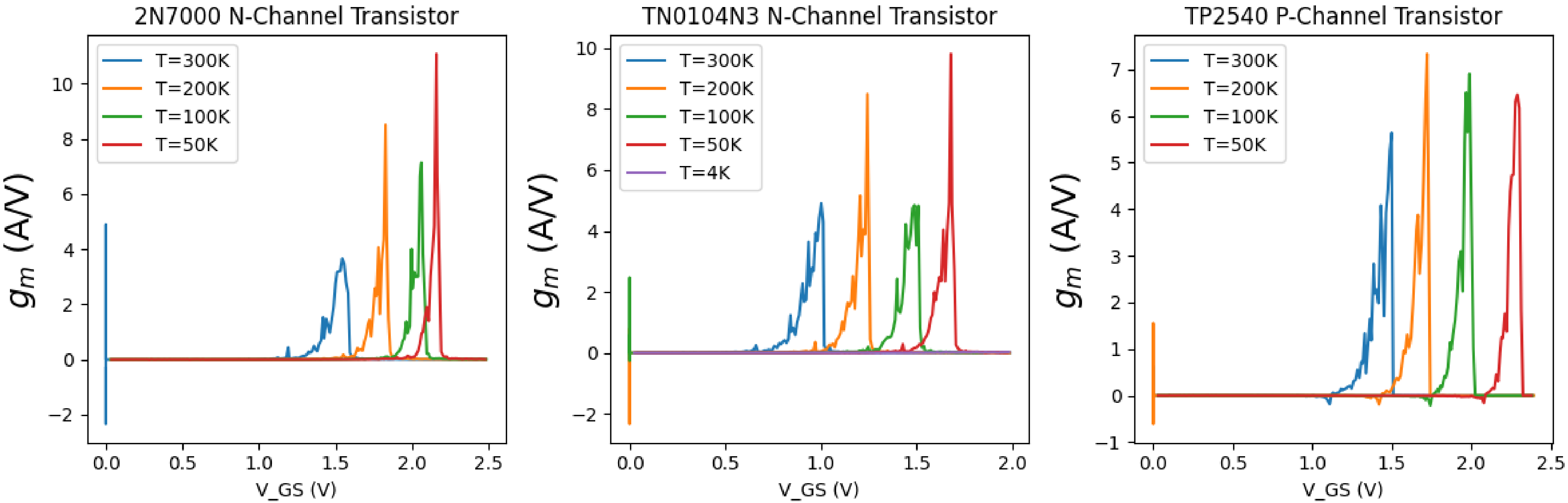

Note for P-MOS, $-V_{GS}= V_{GS}$, we multiplied by -1 when plotting

How to deduce the Subthreshold-Swing vs. Temperature

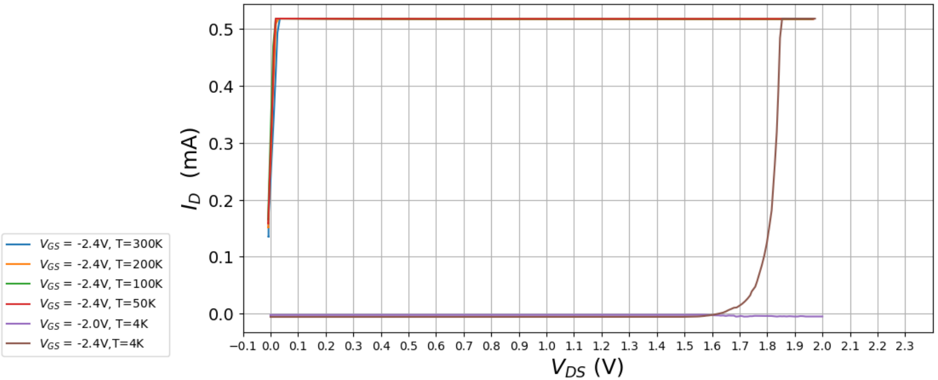

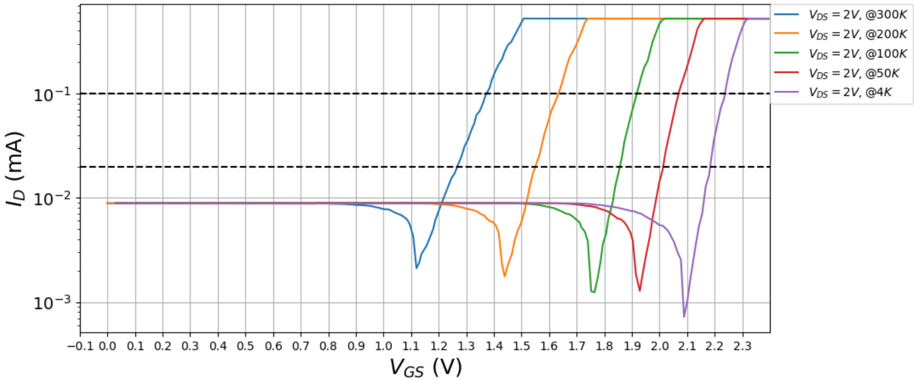

$SS = 143.\frac{mV}{dec}$ T=300K

$114.\frac{mV}{dec}$ $200K$

$114\ \frac{mV}{dec}$ $100K$

$129\frac{mV}{dec}$ $50K$

- The first plot shows the *I-V* plot for a P-type device.
- The second plot shows the $\log(I_D)$ vs. V_{GS}.
- Subthreshold-Swing equation:

$$SS = \left(\frac{d[\log_{10}(I_D)]}{d(V_{GS})}\right)^{-1} * 1000$$

Measured Subthreshold-slope at cryogenic temperatures

- Study of 3 different MOSFET devices 2 N-channel and 1 N-channel.
- See appendix A for *SS* and I-V preliminary data.
- Subthreshold-slope, *SS* vs. *T* in the blue lines.

$$SS = n \ln(10) \frac{kT}{q}$$

- *SS* vs. *T*, scaling factor is on the left side of the plot in the red lines.

$$n = 1 + \frac{C_d}{C_i}$$

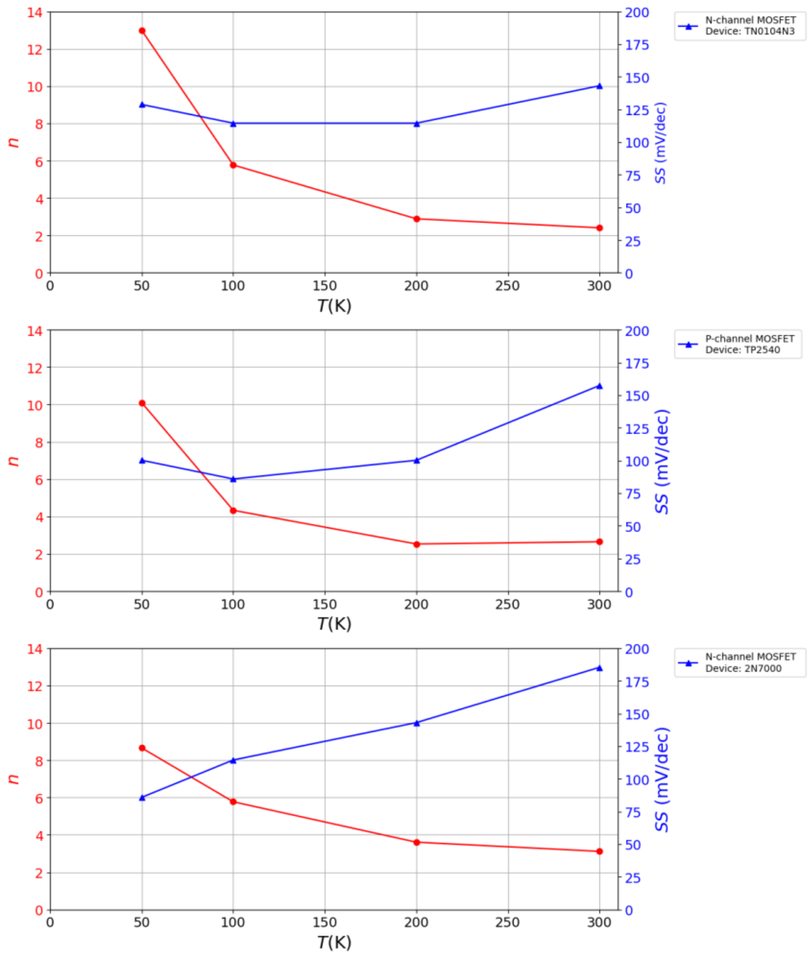

Solving for ϕ_F using depletion width model of MOSFET

- W_M , the depletion width under the channel is defined in terms of ϕ_F , the Fermi potential as

$$W_M = \left(\frac{\epsilon_0 \epsilon_s}{q N_{a,d}} 2|\phi_F|\right)^{\frac{1}{2}}$$

- C_d , the depletion capacitance is expressed in terms of the depletion width as

$$C_d = \frac{\epsilon_0 \epsilon_s}{W_M}$$

- From n, the scaling factor I can deduce the depletion capacitance. Then I plug the new equation for the depletion capacitance. The goal was to isolate ϕ_F since this is needed to get the depletion width.

$$C_d = C_i(n-1)$$

$$\phi_F = \frac{q N_{a,d} W_M^2}{2\epsilon_0 \epsilon_s} = \frac{q \epsilon_s \epsilon_0 N_{a,d}}{2 C_d^2}$$

$$\frac{\phi_F C_i^2}{N_{a,d}} = \frac{q \epsilon_s \epsilon_0}{2(n-1)^2}$$

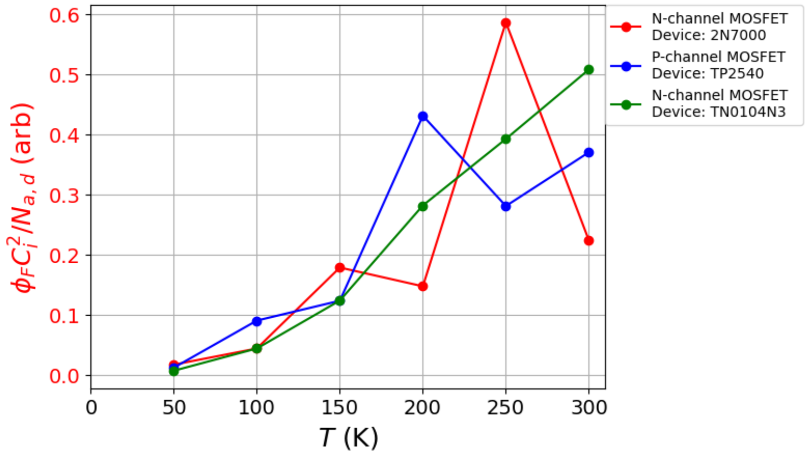

What does the literature say for ϕ_F vs. T?

- Beckers et al. model the Fermi potential ϕ_F vs. T including dopant freezeout. They conclude Fermi potential increase with temperature. This is the text for the figure.

Fermi-Dirac statistics for p from the start: $p = \int g_v(E)[1 - f(E)]dE$, where $g_v(E)$ is the density-of-states in the valence band and $f(E)$ is the Fermi-Dirac distribution function. This exercise was done previously in [34, Sec. 3]. The Fermi level position was calculated numerically using Fermi-Dirac statistics. It was found that in the 0-K limit $E_F \to E_v + (E_A - E_v)/2$ when dopant freezeout is included (E_A is the acceptor dopant energy), while $E_F \to E_v$, when dopant freezeout is not included ($p = N_A$). Typically, $(E_A - E_v)/2 \approx 22.5$ meV is much larger than three times the thermal energy for instance at 4.2 K, $3k_BT \approx 1$ meV. Therefore, the Boltzmann statistics can be assumed for p when dopant freezeout is included, in order to derive an analytical expression for Φ_F^* from $p = N_A^-$:

$$n_i \exp\left(\frac{\Phi_F^*}{U_T}\right) = \frac{N_A}{1 + g_A \exp\left(\frac{\Phi_F^* - \Phi_A}{U_T}\right)} \quad (2)$$

where $\Phi_A \triangleq (E_i - E_A)/q$ (Fig. 3), $U_T \triangleq k_BT/q$ is the thermal voltage, n_i is the intrinsic carrier concentration, and $g_A = 4$ is a degeneracy factor. This gives a quadratic expression for $\exp(-\Phi_F^*/U_T)$ which has the following solution:

$$\Phi_F^* = \underbrace{U_T \ln\frac{N_A}{n_i}}_{\Phi_F} - \underbrace{U_T \ln\frac{1 + \sqrt{1 + (4\alpha N_A)/n_i}}{2}}_{\Delta\Phi_F}, \quad (3)$$

where $\alpha = g_A \exp(-\Phi_A/U_T)$. Φ_A and Φ_F^* are shown in Fig. 5 with solid lines. Φ_F is shown with dotted lines. The function $\Delta\Phi_F = \Phi_F - \Phi_F^*$ measures the difference in Fermi levels at a given T and N_A due to dopant incomplete ionization (freezeout). $\Delta\Phi_F(T, N_A)$ is shown in Fig. 6 versus T for different N_A. As shown in this figure, the maximum of $\Delta\Phi_F$ is around 25 mV. It can be checked that $\lim_{T\to 0} \Delta\Phi_F = \delta/2$ with $\delta = E_A - E_v = 0.045$ eV, for typical, hydrogen-like Si:B doping and thus $\lim_{T\to 0} \Phi_F^* = \Phi_A + \delta/2$ as indicated in Fig. 5. Even though $\Delta\Phi_F$ is in millivolt range, the discrepancy of the predicted current level at threshold can be quite large at cryogenic temperatures, as shown in Fig. 7.

It should be emphasized that in (3), we have obtained $\Phi_F = U_T \ln(N_A/n_i)$ as part of the expression of Φ_F^*. $\Phi_F = U_T \ln(N_A/n_i)$ would be obtained when assuming Boltzmann statistics for p and complete ionization for N_A, which we knew was not valid because $E_F \to E_v$ in that case. However, Φ_F can be used here, because Φ_F is just a part of the derived expression for Φ_F^*, which has nothing to do with the validity of the Boltzmann statistics anymore.

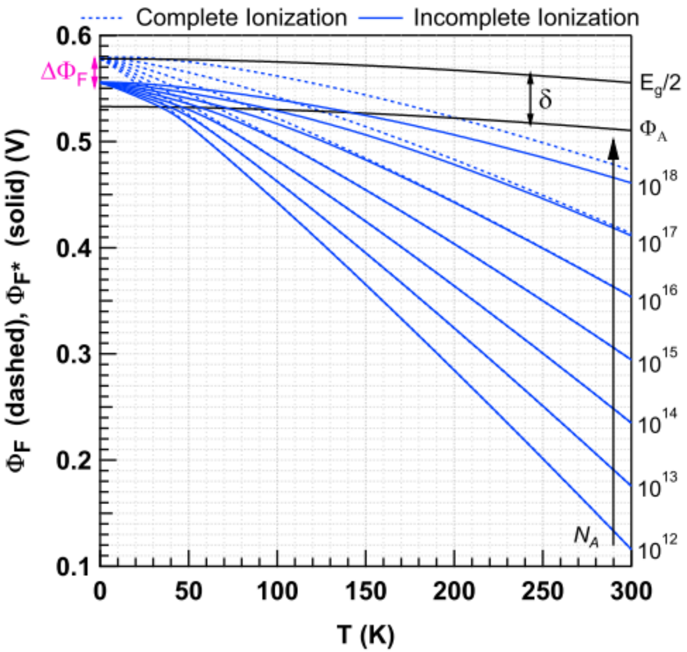

Citation: A. Beckers, F. Jazaeri, A. Grill, S. Narasimhamoorthy, B. Parvais and C. Enz, "Physical Model of Low-Temperature to Cryogenic Threshold Voltage in MOSFETs," in *IEEE Journal of the Electron Devices Society*, vol. 8, pp. 780-788, 2020

Appendix A.1

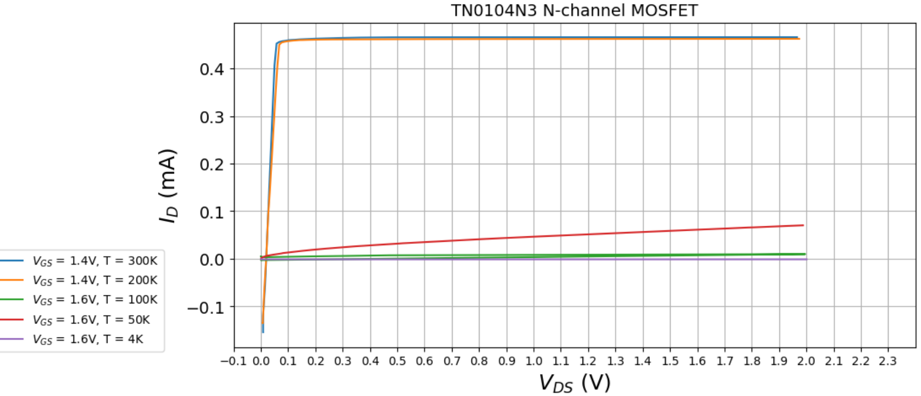

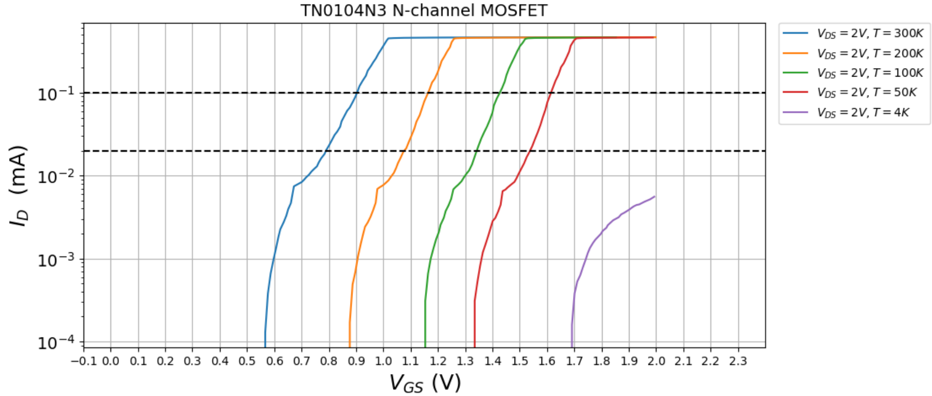

- I-V Measurements for n-type device and Subthreshold-Swing.

$SS = 143.07\frac{mV}{dec}$, T=300K

$114.45\frac{mV}{dec}, 200K$

$114.45\frac{mV}{dec}, 100K$

$128.76\frac{mV}{dec}, 50K$

Appendix A.2

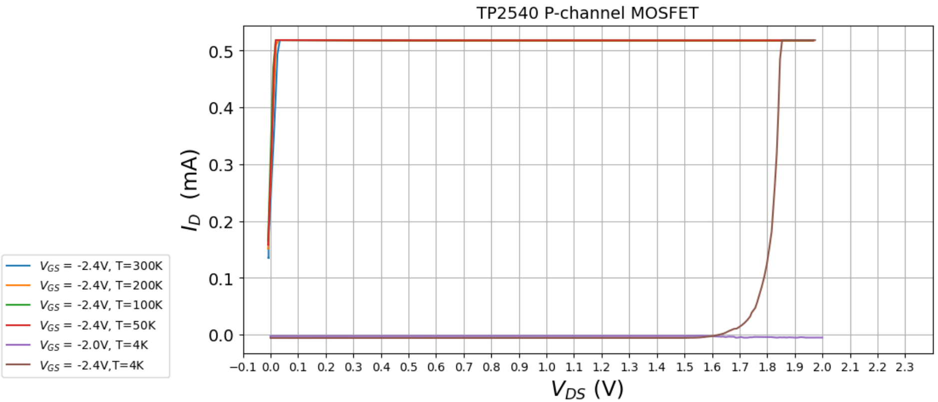

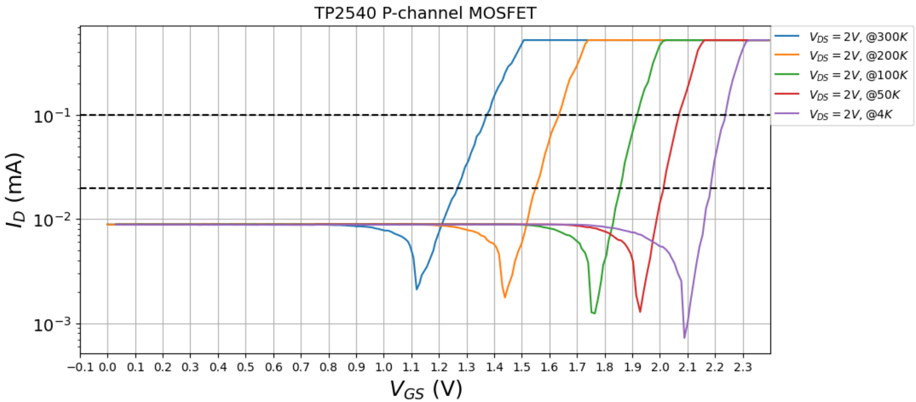

- I-V Measurements for p-type device and Subthreshold-Swing.

$SS = 157.37\frac{mV}{dec}$,T=300K

$100.14\frac{mV}{dec}, 200K$

$85.84\frac{mV}{dec}, 100K$

$100.14\frac{mV}{dec}, 50K$

$71.53\frac{mV}{dec}, 4K$

Appendix A.3

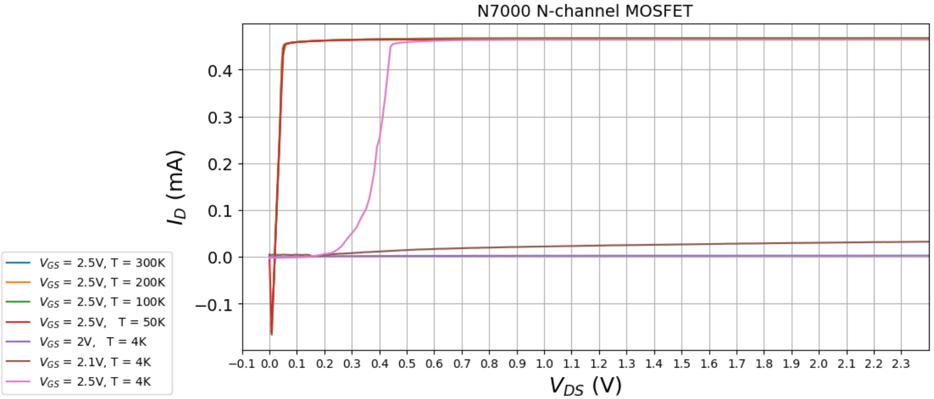

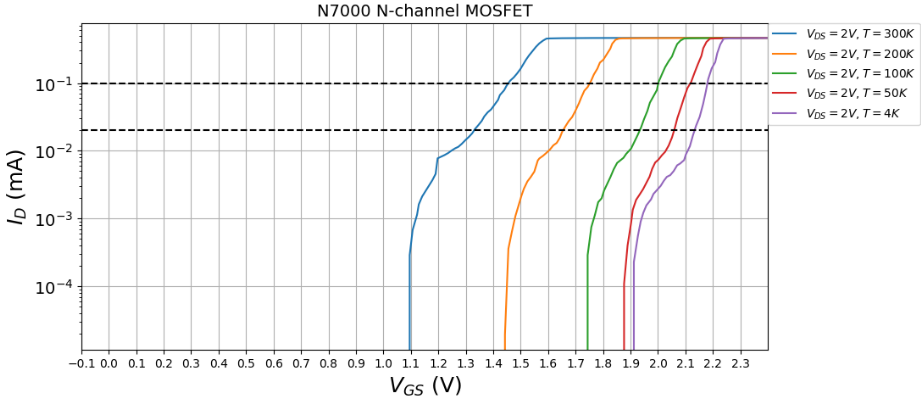

$SS = 185.98\frac{mV}{dec}$, T=300K

$143.06\frac{mV}{dec}, 200K$

$114.45\frac{mV}{dec}, 100K$

$85.84\frac{mV}{dec}, 50K$

$85.84\frac{mV}{dec}, 4K$

- I-V Measurements for n-type device and Subthreshold-Swing.

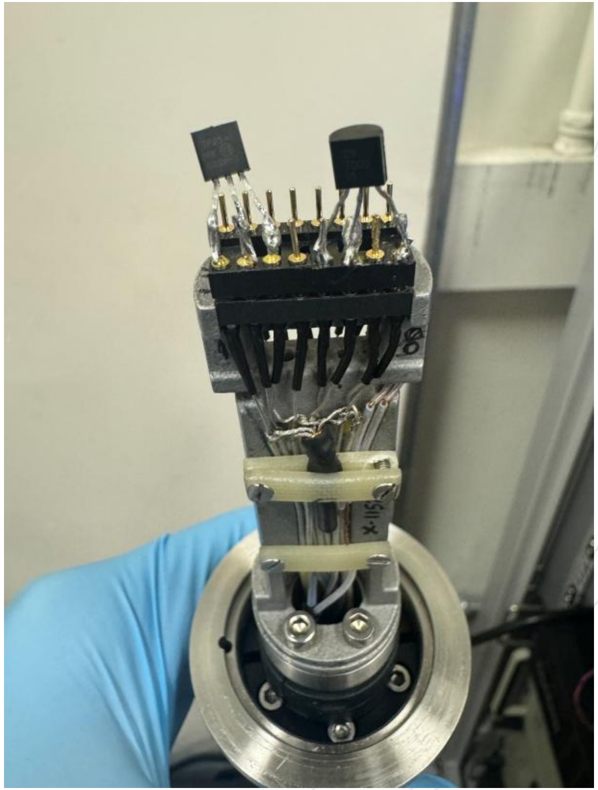

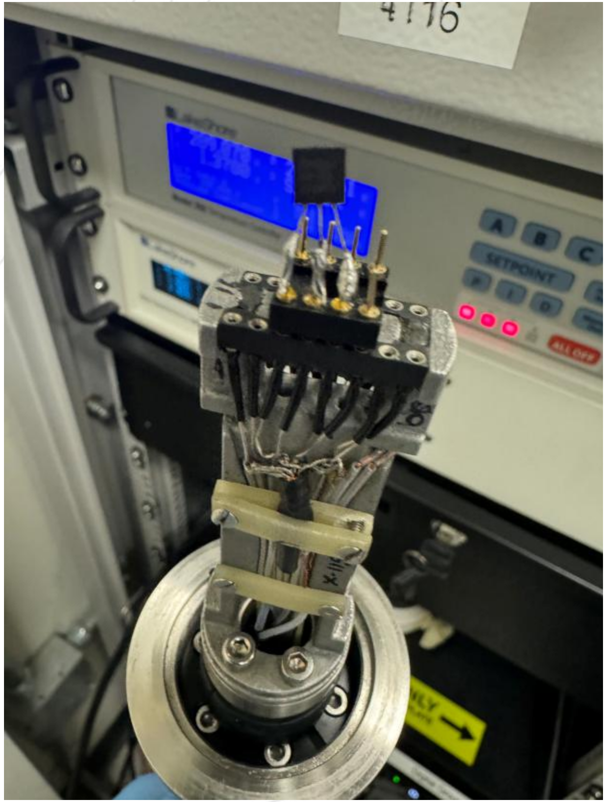
4116
A
B
C
SETPOINT
ALL OFF